ASYMMETRIES IN DEEP INELASTIC SCATTERING

E. Gabathuler

JOURNAL DE PHYSIQUE
Colloque C2, supplément au n°2, Tome 46, février 1985

ASYMMETRIES IN DEEP INELASTIC SCATTERING

E. Gabathuler

Oliver Lodge Laboratory, University of Liverpool, U.K.

Résumé - Nous faisons une revue des données existantes sur les asymétries dans la diffusion profondément inélastique avec un changement des hélicités du quark et du lepton. Nous discutons l'état actuel de l'expérience E.M.C. sur les fonctions de structure de spin ainsi que les développements futurs.

Abstract - We review the existing data on asymmetries in deep inelastic muon scattering involving changes in the lepton and quark helicities. The status of the present E.M.C. experiment on spin structure functions is discussed together with future developments.

The process of Deep Inelastic Scattering using electron, muon and neutrino probes has been very successful in developing our present understanding of the role of quarks and gluons in strong interactions. This knowledge has been obtained mainly from measurements of the scattering cross-section which determine the structure functions over a wide kinematic range. Precise measurements of the structure functions using muon beams provided evidence that Λ related to α_s, the strong coupling constant was small (1) and that quarks behaved differently in bound and free nucleons, the E.M.C. effect (2). The extension of these experiments to those where the lepton and/or quark spin is defined in the initial state provide additional new information as highlighted by experiments on weak electromagnetic interference. In this lecture, we shall review the current status of these experiments and indicate what new information can be expected in the future from muon experiments.

The kinematics of the deep inelastic scattering process are illustrated in fig. 1. For an incident muon of energy E and scattered energy E' and scattered angle θ, we can define the following variables.

$$Q^2 = 4EE' \sin^2\theta/_2 = EE'\theta^2 \text{ (small } \theta)$$

$$\nu = E - E'$$

and the scaling variables $x = Q^2/2m\nu$ and $y = \nu/E$. For a fixed incident energy, low Q^2 corresponds to small scattering angles and as Q^2 increases we move into a region of larger x and larger y in the kinematic plot.

The muon beam is naturally polarised since the muons are produced by the weak decay of pions in flight. It is easy to produce a highly polarised beam of μ_L^+ from $\pi^{+,s}$ by selecting forward $\pi \to \mu$ decays in the pion centre of mass, i.e., muons of energy close to that of the parent pions. The effect of tuning the muon beam momentum to maximise the beam polarisation is illustrated in fig. 2(a) and the corresponding reduction of the muon flux is shown in fig. 2(b). A beam of μ_R^+ of approximately half the pion energy can be made from $\pi^{+,s}$ by selecting backward $\pi \to \mu$ decays in the pion centre-of-mass. Unfortunately for the same incident pion flux, the μ_R^+ beam has only 10% of the μ_L^+ intensity for the same momentum bite, and therefore many more protons are required for a μ_R^+ beam. The simplest method of producing a μ_R beam is to use forward μ^- decays from an incident π^- beam. However we have to consider any additional asymmetry introduced by the change in sign of the charge as well as the helicity.

Although it is possible to calculate the polarisation of the muon beam, it

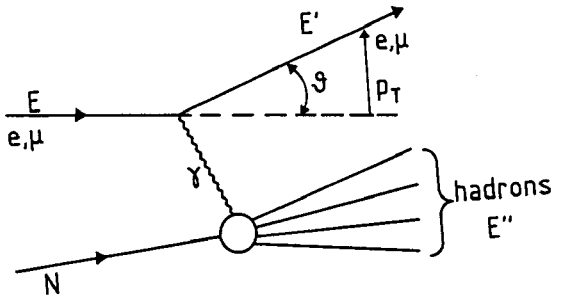

$Q^2 \simeq EE'\,\vartheta^2 \simeq E p_T^2/E'$

$\nu = E_{had} = E - E'$

$x = Q^2 / 2M_N \nu$

$y = \nu / E$

Fig. 1. Kinematics of Deep Inelastic Scattering.

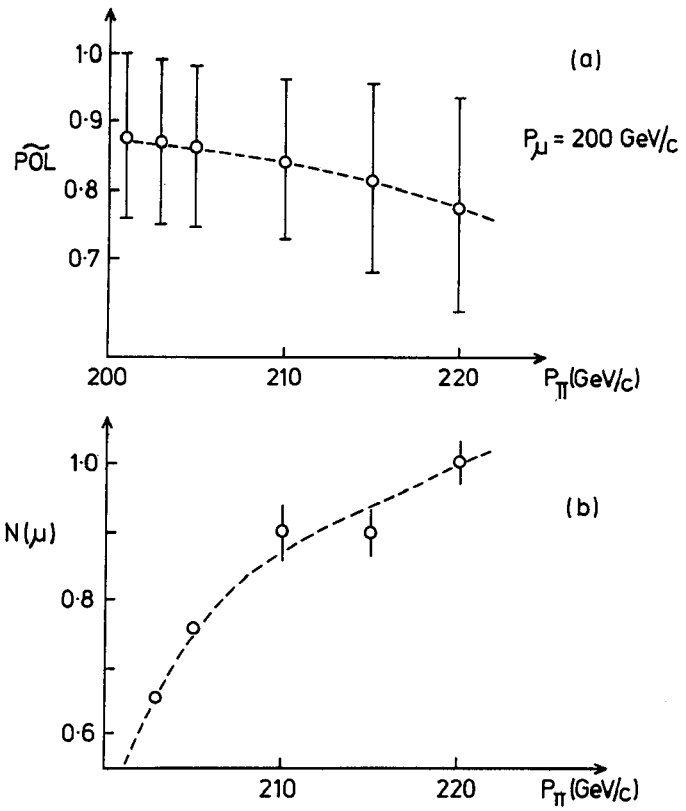

Fig. 2. (a) The mean polarisation versus pion momentum for a muon momentum of 200 GeV/c.

(b) The muon flux versus pion momentum for a muon momentum of 200 GeV/c.

is nevertheless essential to measure it in the experiment since the polarisation can change due to our lack of understanding of the kaon background in the pion beam and the muon energy loss in magnetic collimators which determine the momentum spread of the muon beam. The muon polarisation can be determined using the $\mu \to e$ decay process where the polarisation is measured from the energy spectrum of the decay electrons as illustrated in fig. 3. Previous measurements have been carried out by the B.C.D.M.S. Collaboration (3) and these are in agreement with the calculated value to within 10%. For the present E.M.C. experiments, we plan to measure the polarisation to a precision of 5% at 100 and 200 GeV/c muon momenta.

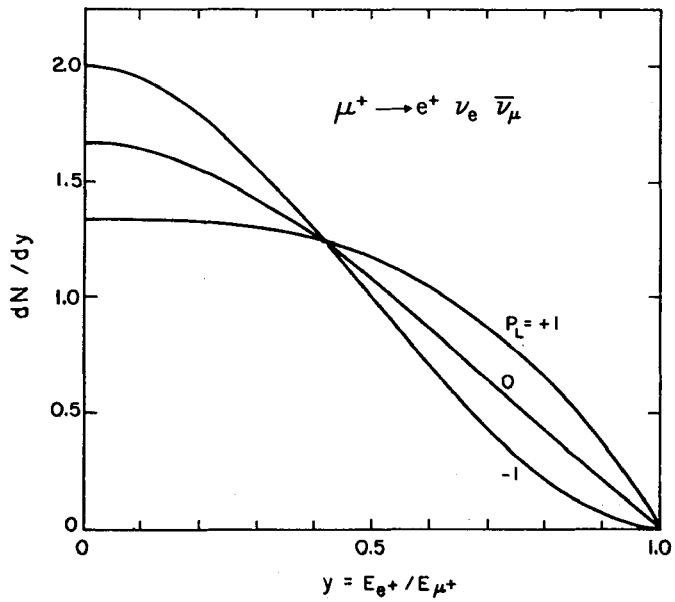

Fig. 3 The electron energy spectrum in muon decay for different values of the muon polarisation. Maximum sensitivity at y = 0.75.

In deep inelastic scattering, asymmetries can arise by changing the sign or the polarisation of the lepton or by changing the polarisation of the nucleon (quark) or both. We shall first consider what happens when we change the sign of the charge of the lepton. Here an asymmetry can arise due to the interference between the normal one photon exchange process and the two photon exchange process. The cross-section can be written in terms of the charge e_μ as

$$\sigma(\mu^\pm) = |e_\mu|^2 + |e_\mu|^4 \pm I(e_\mu^3)$$

where the last term is the interference term which changes sign when the sign of the muon charge is changed. The asymmetry $A^\pm$ measures the deviation introduced by the presence of any two photon exchange contributions. The results are usually plotted as a function of υ since any effect should have a log υ or a υ log υ behaviour. The results of an experiment carried out by the B.C.D.M.S. Collaboration are presented in fig. 4 and show that there is no evidence for any two photon exchange effects. However radiative corrections should be applied to any experimental result when the helicity is changed by changing the sign of the charge.

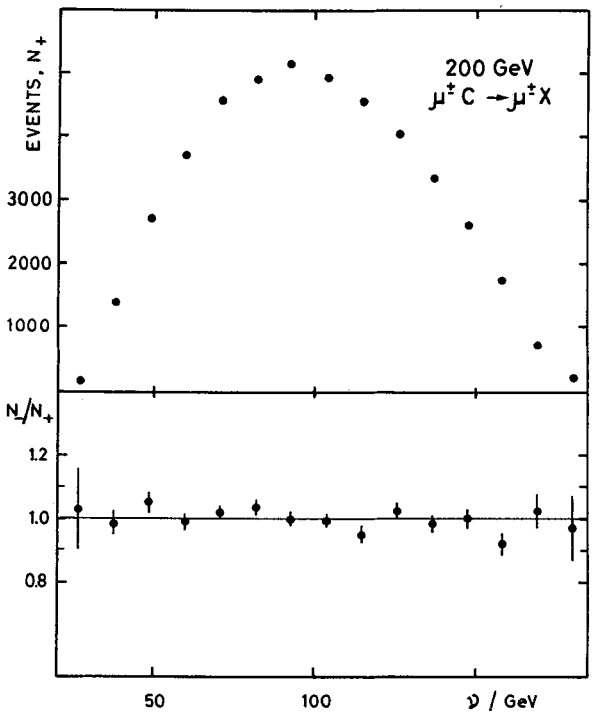

Fig. 4 The ratio of deep inelastic scattered events for μ^- and μ^+ beams versus ν.

The helicity asymmetry provides a sensitive measurement of the effect of the weak interaction brought about by replacing the photon propagator by the Z^o boson propagator for neutral current processes. Fig. 5 shows the relationship between

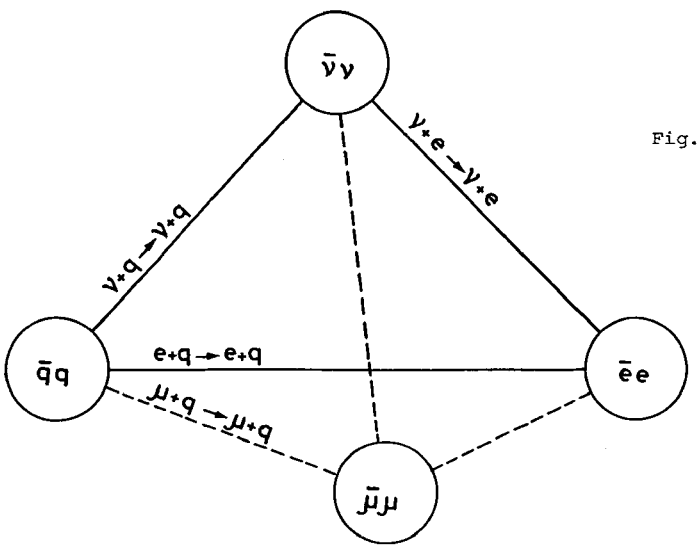

Fig. 5 The relationship of the different leptonic processes connecting the Z^o propagator to those leptons.

the different leptonic and quark weak processes. The electron and muon quark scattering processes (i.e. deep inelastic scattering) provide an important link between all the various leptonic and quark weak processes. The magnitude of the interference term is given by:

$$\frac{d\sigma^{\mp}_{\gamma Z}(\lambda)}{} = \frac{G_F}{\sqrt{2}} \frac{\alpha}{Q^2 2} \left[1 + (1-y)^2\right] G_2(x) \left\{-v_\mu \pm \lambda a_\mu\right\}$$

$$+ \left[1 + (1-y)^2\right] x G_3(x) \left\{\pm a_\mu - \lambda v_\mu\right\}$$

when v_μ and a_μ are the standard vector and axial couplings and λ is the muon helicity. $G_2(X)$ and $G_3(X)$ are the interference structure functions analogous to $F_2(X)$ and $xF_3(x)$ in neutrino scattering. If we change the helicity of the beam (holding the charge fixed), then the asymmetry is given by

$$A^{\mp}(\lambda_1, \lambda_2) = \left\{\sigma^{\mp}_{\gamma,Z}(\lambda_1) - \sigma^{\mp}_{\gamma,Z}(\lambda_2)\right\} \Big/ 2\sigma_0$$

$$= -KQ^2 \left\{\frac{\lambda_1 - \lambda_2}{2}\right\} \left\{v_\mu A\, g(y) \mp a_\mu V\right\}$$

when $K = 1.8\ 10^{-4}\ \text{GeV}^{-2}$ and A and V are related to the weak quark couplings. The A^- asymmetry is given by

$$A^-(\lambda_1, \lambda_2) \approx 10^{-4} Q^2$$

which is therefore very small, ~1% even at $Q^2 = 100\ (\text{GeV/c})^2$. The A^+ term is not sensitive to $\sin^2\theta_W$ due to the near cancellation of the two terms in the above expression.

If we now change the beam helicity and the charge simultaneously as for example $\mu^+_L \to \mu^-_R$, then we can define a new asymmetry.

$$B(\lambda_1, \lambda_2) = -KQ^2\, g(y) \left\{a_\mu - \lambda v_\mu\right\} A$$

$\lambda_1 = |\lambda|$ ------ μ^-_R

$\lambda_2 = -|\lambda|$ ------ μ^+_L

The B asymmetry is a factor of two larger than the A asymmetry and is essentially parity conserving since V_μ is very small. The A asymmetry is parity violating as it involves vector-axial combinations.

The B asymmetry is relatively easier to measure since by reversing the sign of the muon beam, the energy is unchanged and we only lose a factor of 3 in the muon intensity.

An experiment has been carried out by the B.C.D.M.S. Collaboration (4) to measure the B asymmetry using the apparatus illustrated in fig. 6. The apparatus consists of ten iron toroids magnetised to saturation containing ten target sections 5 metres long. Scintillation hadoscopes and proportional chambers are placed along the length of the modules to trigger the apparatus and to track the helical path of the scattered muon. Data were taken at 120 and 200 GeV, where the lower energy data have been used mainly to provide cross-checks on systematic errors and radiative corrections. The results of the B asymmetry are illustrated in figs. 7 and 8 and show excellent agreement with the S-W-G model of the electroweak interaction (5). The importance of controlling systematic errors is clearly indicated in fig. 8 where the effect of a 0.3% change in the absolute determination of the spectrometer field or in the difference of the μ^+ and μ^-

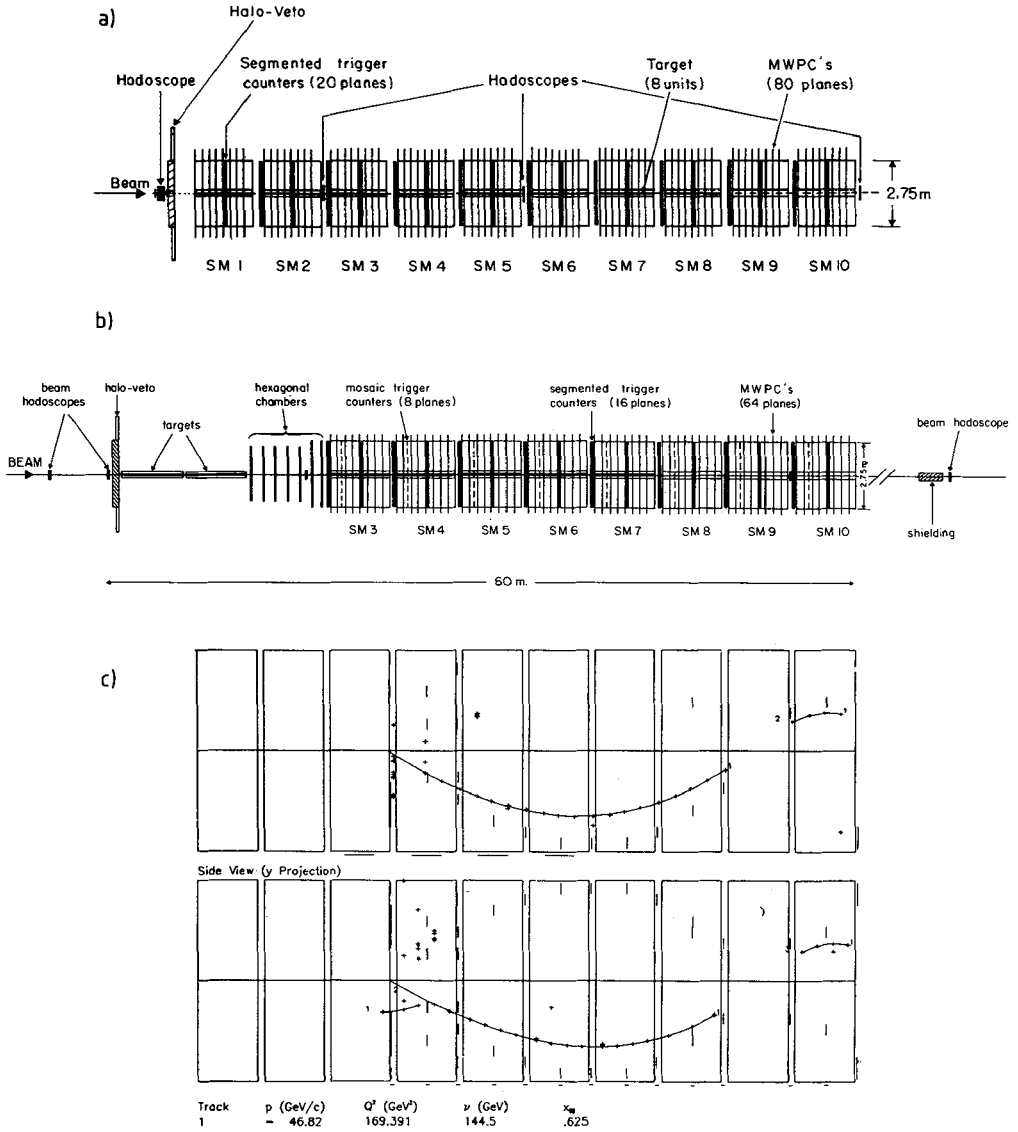

Fig. 6 The muon spectrometer of the B.C.D.M.S. Collaboration (NA4 experiment).

momenta is clearly seen to have a large effect on the asymmetry. The data have been used to determine

$$\sin^2\theta w = 0.23 \pm 0.07 \text{ (STAT)} \pm 0.04 \text{ (SYST)}$$

The possibility of carrying out future experiments to measure $\sin^2\theta w$ with an overall precision of 0.01 is very difficult using muon beams when both statistical and systematic errors are taken into account. It is certainly possible to increase the size of the effect by extending Q^2, but we are only able

to gain at most a factor of 2 with present and future fixed target accelerators. New experiments using neutrino beams offer the best hope of achieving high precision in the determination of $\sin^2\theta_W$ at $Q^2 \ll M_Z^2$. Unless some new feature of the higher order weak contribution arises which would make muon-quark interaction unique, then we do not see any physics argument to pursue any further measurements on the weak asymmetries using muon beams.

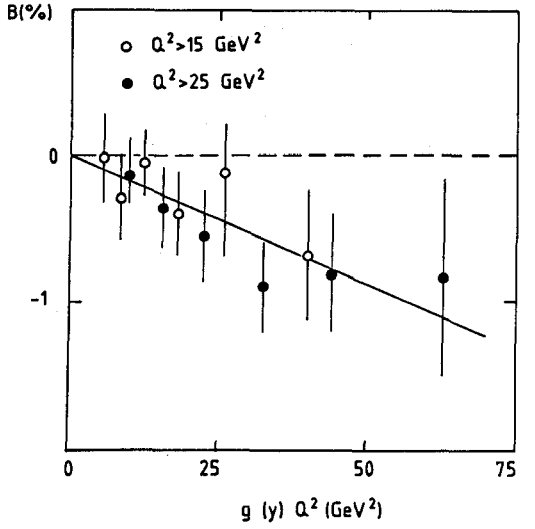

Fig. 7 The B_μ asymmetry versus $g(y)\ Q^2$ $(GeV)^2$ measured by the NA4 experiment at $E_\mu = 120$ GeV.

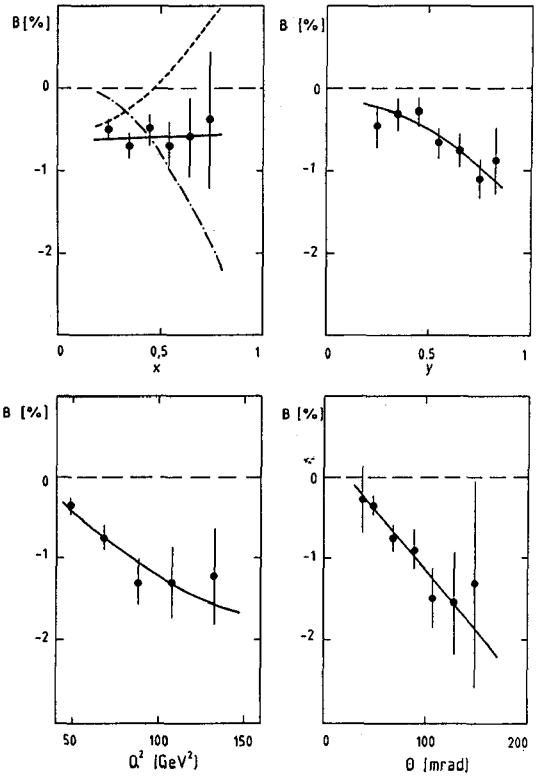

Fig. 8 The B_μ asymmetry at $E_\mu = 200$ GeV plotted as a function of x, y, Q^2 and θ. The dashed and dotted lines are explained in the text.

We shall now consider quark asymmetries where the proton is longtitudinally polarised. The cross-section for unpolarised muon-proton inelastic scattering is given in terms of the $W_1(Q^2,\nu)$ and $W_2(Q^2,\nu)$ structure functions by

$$\frac{d^2\sigma}{d\nu dE'} = \left(\frac{d\sigma}{d\nu}\right)_{MOTT} \left\{ W_2(Q^2,\nu)\cos^2\theta/2 + 2W_1(Q^2,\nu)\sin^2\frac{\theta}{2} \right\}$$

If we now differentiate between the two spin states of the initial proton, then we can define two additional spin-dependent structure functions $G_1(Q^2,\nu)$, $G_2(Q^2,\nu)$

$$\frac{d^2\sigma}{d\nu dE'} = \left(\frac{d\sigma}{d\nu}\right)_M \left\{ W_2 + 2\tan^2\frac{\theta}{2}\cdot W_1 + 2\tan^2\frac{\theta}{2}\left[E+E'\cos\theta\right] M G_1 + 8EE'\tan^2\theta/2\,\sin^2\theta/2\, G_2 \right\}$$

The spin dependent structure functions can be isolated by using the cross-sections for lepton-nucleon spins parallel ($\uparrow\uparrow$) and anti-parallel ($\uparrow\downarrow$).

$$\frac{d^2\sigma}{d\nu dE'}(\uparrow\downarrow) - \frac{d^2\sigma}{d\nu dE'}(\uparrow\uparrow) = \frac{4\alpha}{Q^2}\frac{E'}{E}\left\{ M G_1(E-E'\cos\theta) - Q^2 G_2 \right\}$$

The scaling variables $g(x,Q^2)$ are similar to $F(x,Q^2)$ and are given by

$$M^2\nu G_1(Q^2,\nu) = g_1(x,Q^2)$$
$$M\nu^2 G_2(Q^2,\nu) = g_2(x,Q^2)$$

If we now define the asymmetry

$$A = \frac{d\sigma(\uparrow\downarrow) - d\sigma(\uparrow\uparrow)}{d\sigma(\uparrow\downarrow) + d\sigma(\uparrow\uparrow)} = D\left\{ A_1^P + \eta A_2^P \right\}$$

where

$$A_1^P = \frac{\sigma_{1/2} - \sigma_{3/2}}{\sigma_{1/2} + \sigma_{3/2}} = \frac{M\nu G_1 - Q^2 G_2}{W_1}$$

and

$$A_2^P = \frac{2\sigma_{TL}}{\sigma_{1/2} + \sigma_{3/2}} = \frac{\sqrt{Q^2}}{W_1}(M G_1 + \nu G_2)$$

$\sigma_{1/2}$ and $\sigma_{3/2}$ are the virtual photon-proton cross-sections for total spin of $^1/_2$ and $^3/_2$. σ_T (σ_L) is the transverse (longtitudinal) photon cross-section. D and η are kinematical factors when $D(y) = \frac{1-(1-y)^2}{1+(1-y)^2}$ is the virtual photon depolarisation factor varying between 0 and 1.0 as y varies from 0 to 1.0. η is given by $\eta = \frac{2(1-y)}{1-(1-y)^2}\frac{\sqrt{Q^2}}{E}$ and is very small in the kinematic range of the experiments. This means that the A_1 term is dominant, which corresponds to the longtitudinal spin measurements.

$$A_1^P(x,Q^2) \approx \frac{2x\, g_1^P(x,Q^2)}{F_2(x,Q^2)}\left[1+R\right]$$

$A_1(x,Q^2)$ is model dependent and can be predicted using various assumptions on how the spin of the proton is taken up by the quarks.

It is possible to calculate precisely a sum rule for polarised structure functions. The Bjorken Sum rule (6) is given by:

$$\int_0^1 \frac{dx}{x}\left[\left\{\frac{A_1^p(x).F_2^p(x)}{1+R^p}\right\} - \left\{\frac{A_1^n(x).F_2^n(x)}{1+R^n}\right\}\right] = \tfrac{1}{6}\frac{g_A}{g_V}$$

$$A_1^n(x)\,F_2^n(x) \ll\ll A_1^p(x)\,F_2^p(x)$$

$$\therefore \int \frac{dx}{x}\,\frac{A_1^p(x)\,F_2^p(x)}{1+R^p} \approx \int_0^1 \frac{dx}{x}\,A_1(x)\,F_2(x) = 0.418 \pm 0.002$$

It is interesting to note that the sum rule is heavily weighted to small x by the $1/x$ term and therefore the measurements of $A_1(x)$ should extend down to very small x.

A second sum-rule is given by Ellis-Jaffe (7)

$$2\int_0^1 g_1^p(x)\,dx = \frac{0.89}{3}\cdot\frac{g_A}{g_V} = 0.372 \pm 0.002.$$

The spin polarisation structure functions $g(x,Q^2)$ are expected to show similar scaling deviations at large and small x as given by F(x). These have been calculated in Q.C.D. by Darrigol and Hayot (8) and the prediction for g(x) and A(x) are illustrated in fig. 9. From these curves it will be very difficult to measure scaling violations in a single experiment.

The only experiments which have been completed so far on polarised structure functions have been carried out by a Yale-SLAC Collaboration at SLAC using polarised electrons of 22.6 and 16.2 GeV (9). These experiments are very difficult since the measured asymmetry A_1^M is very much smaller than the true asymmetry A_1.

$$A_1^M = P_B\,P_T\,\tilde{D}\,f\,A_1$$

when P_B and P_T are the beam and target polarisations, f is the free proton content of the target and $\tilde{D}$ is the kinematic depolarising factor referred to earlier. The difference between the measured asymmetry and the true asymmetry depends on the kinematics, but can be as large as 100. The uncertainty in the asymmetry is given by

$$\Delta A_1 = \left\{\frac{1}{(P_B P_T D f)^2.N} + 0.005\,A_1^2\right\}^{1/2}$$

where N is the number of events and a 5% uncertainty has been taken for P_B and P_T. We should therefore endeavour to enhance all the various factors P_B, P_T and f to the largest possible values and control the systematic errors in the experiment. The results of the SLAC experiment for the A_1 asymmetry are illustrated in fig. 10 showing that the asymmetry increases towards unity at large x. The predictions of various models are also illustrated in fig. 10. The spin-dependent structure function $g_1^p(x)$ is plotted versus x in fig. 11 where the value of $F_2(x)$ was taken from a Burâs-Gaemers parameterisation (10) and R was taken as 0.25. The data covering the x range ($0.1 \lesssim x \lesssim 0.65$) do not show any Q^2

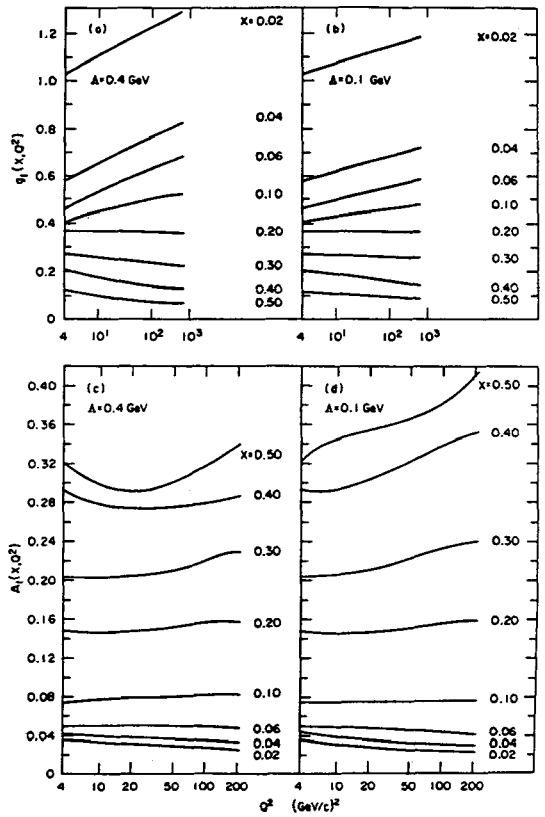

Fig. 9 The theoretical Q.C.D. predictions for $g_1(x,Q^2)$ and $A_1(x,Q^2)$ versus Q^2 for two different values of Λ.

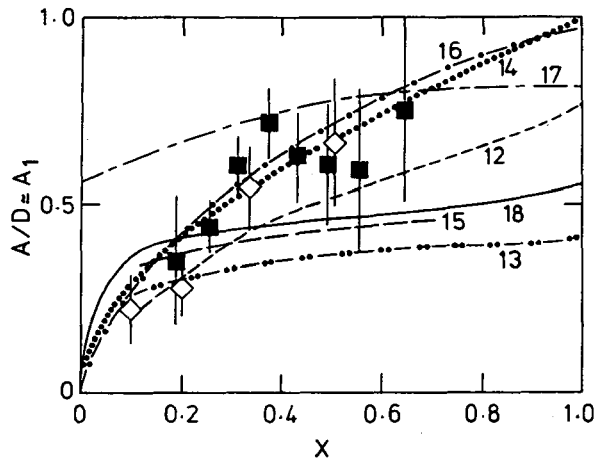

Fig. 10 The value of the A_1 asymmetry plotted against x as measured by the S.L.A.C.-Yale group.

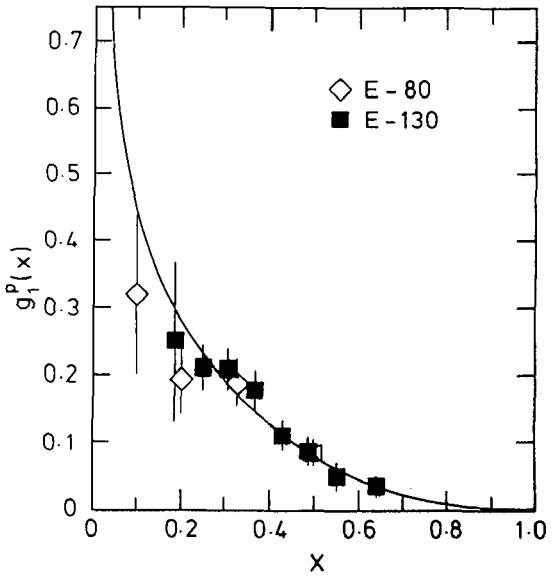

Fig. 11 $g_1^p(x)$ plotted against x for the S.L.A.C.-Yale experiment. The solid curve is a fit to the data given by $A_1 = 0.94\ x^{1/2}$.

dependence over the limited Q^2 range ($1 \leq Q^2 \leq 10$) $(GeV/c)^2$. The data have been used to test the Bjorken sum rule and this is illustrated in fig. 12. However since the data are predominantly at large x, the sum rule integration covered by the experimental data is much less than half of the total weighted sum. From this plot, we can see the importance of extending measurements to small x.

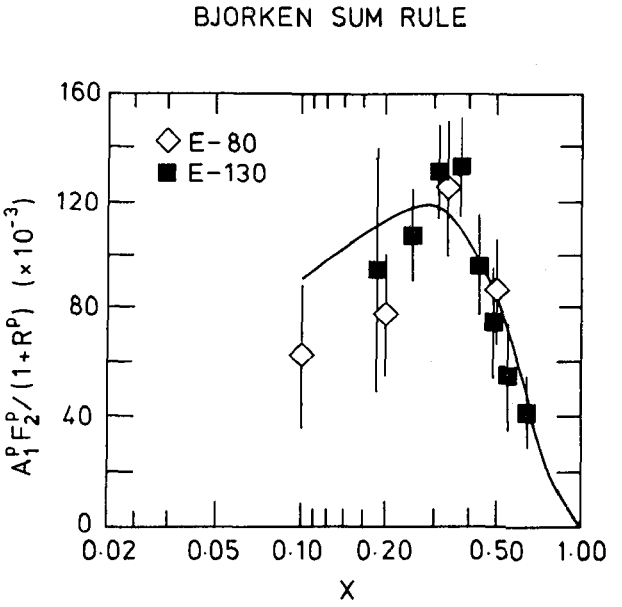

Fig. 12 The measurement of the Bjorken sum rule given by the S.L.A.C.-Yale data.

The E.M.C. experiment has taken data using a polarised target this year. We have collected one million good reconstructed events (assuming 10% of all triggers produce good events) at an incident muon energy of 200 GeV and half a million good events at 120 GeV. The beam intensity passing through the polarised target was 3 x 10^7 μ's/spill. The Q^2 range has been extended up to ~50 $(GeV/_c)^2$ and the x range has been extended down to 0.015.

The polarised target contains NH_3 which has the highest free proton content of 17.5% and has the remarkable property that a high polarisation of $\gtrsim$ 80% can be achieved after irradiation (11). In the experiment to measure the structure functions $F_2(x,Q^2)$, we had found that the largest source of systematic errors arose from time variations of the beam and the measuring apparatus (mainly wire chambers). The polarised target was therefore split into two sections of 40cm along the beam line and the two cells were polarised in opposite directions. The targets were separated by 20cms to enable a clean separation of the two classes of events (↑↑ + ↑↓) and the two spin configurations were recorded simultaneously in the detection apparatus. The direction of the spin was interchanged in the two targets at least once per running period to reduce any systematic effects due to filling factors, geometry and acceptance.

The measurement of the kinematics of the scattered muon were made using the standard E.M.C. spectrometer illustrated in fig. 13 to which additional chambers have been added to improve the reconstruction of the scattered muon back into the target cells. The apparatus consists of a large dipole magnet with drift chambers placed on either side to measure the trajectory of the scattered muon. Scintillation counter hodoscopes are used to trigger the experiment and to veto unwanted halo muons which are not in the beam.

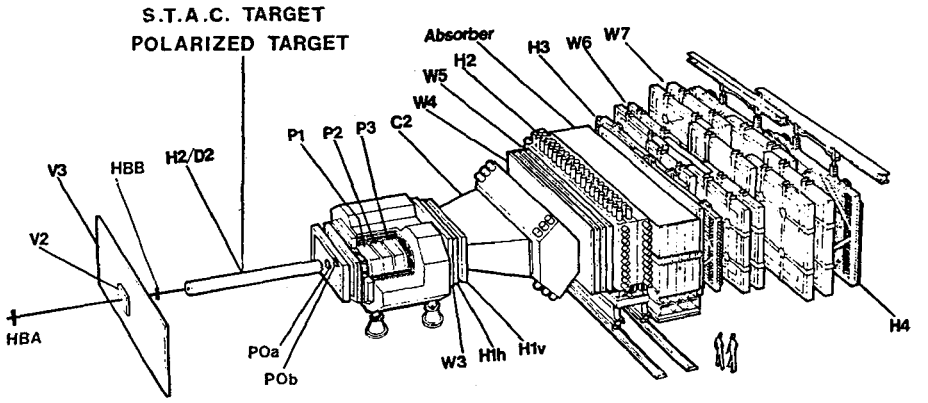

Fig. 13 The muon spectrometer of the E.M.C. collaboration.

As we have just finished running very recently, we are unable to provide any results at this conference since there is quite an involved procedure requiring alignment of the detection planes, efficiency determinations, geometry and kinematics to be gone through before it is possible to produce physics. However in order to give an indication of what the data should look like we have used the present statistics to simulate the results. The errors are purely statistical since we cannot predict the size of the systematic errors until all the data have been analysed.

The results of this simulation are illustrated in fig. 14 for the A_1 asymmetry, in fig. 15 for the structure function $g_1(x,Q^2)$ and in fig. 16 for the Bjorken sum rule for A_1^p. From this simulation we can see that it should be

possible to make a more precise test of the models for the asymmetry A_1, but it will be difficult to determine a Q^2 dependence for A_1 or $g(x,Q^2)$ unless we can combine the E.M.C. and SLAC data. We should be able to provide a good test of the Bjorken sum rule. However we have to stress that we have performed our simulation bases on an extrapolation of the existing SLAC results and that the size of the systematic errors will be crucial in deciding the overall quality of the data.

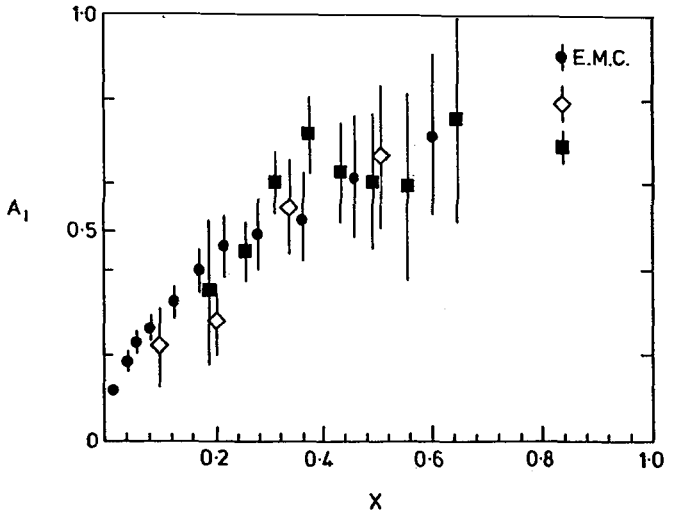

Fig. 14 The "predicted" data of the E.M.C. experiment for the A_1 asymmetry versus x. The errors are based on the statistics taken in 1984.

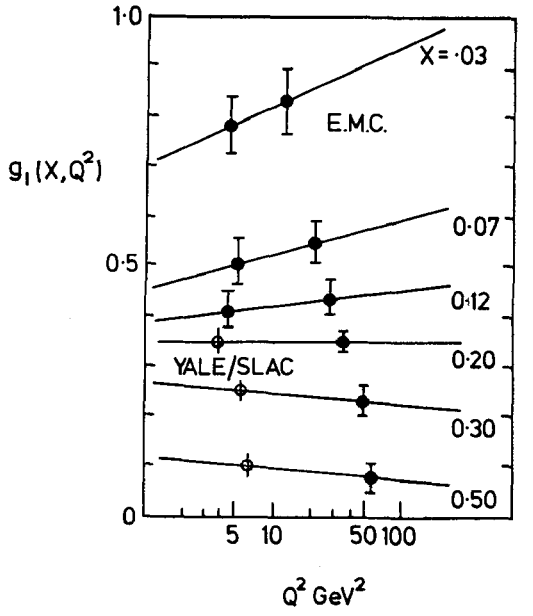

Fig. 15 The "predicted" E.M.C. data for the measurement of $g_1(x,Q^2)$ versus Q^2.

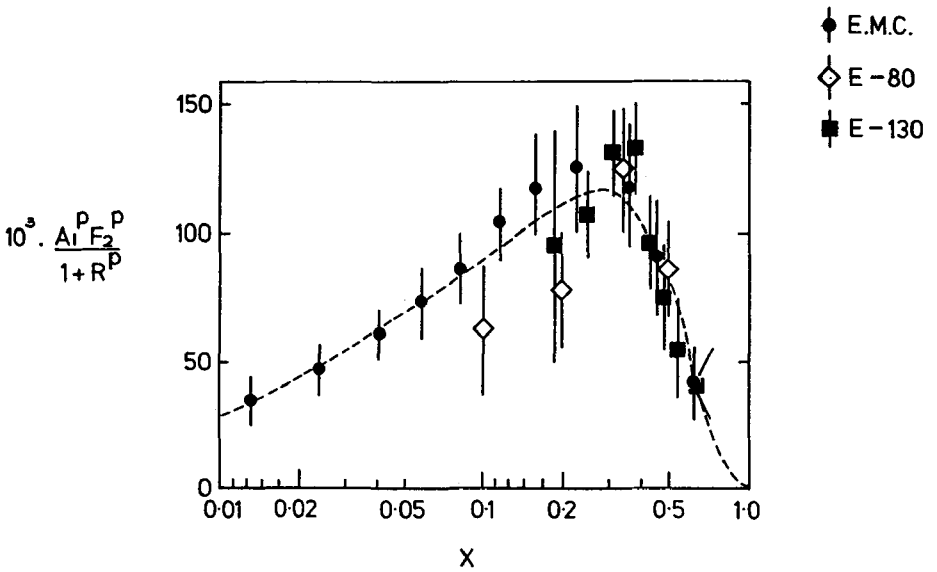

Fig. 16 The "predicted" E.M.C. data for the Bjorken sum rule.

We intend to take more data with the polarised target in 1985, but here the running will be divided between a more detailed study of the E.M.C. effect using heavy targets and the polarised target. It will be difficult to increase the present statistics by more than 50%, but this data will be very important to help our understanding of the systematic errors when compared with the 1984 data. Clearly it would be very beneficial to improve the statistical accuracy of the experiment by an order of magnitude assuming that the systematic errors can be kept under control. However we do not believe that this is feasible with the present apparatus or muon beam. A measurement of $A_2(x,Q^2)$ using tranversely polarised quarks would be very interesting, but this again is difficult to achieve with a muon beam. We also believe that it would be very useful to have a measurement of the fundamental quantity A_1^n for the neutron. Such an experiment requires a polarised deuteron target which only produces neutrons polarised to the order of 30%. This measurement should be carried out at SLAC, where the lower energy is well matched to the larger x region where A_1^n is expected to be non-zero and where the intensity can be increased provided the target can be developed to handle the rate. We believe that this measurement should be made at some time in the future.

References

(1) Aubert, J.J. et al., Phys. Lett., 105B, (1981), 322.
Bollini, D. et al., Phys. Lett., 104B, (1981), 403.
(2) Aubert, J.J. et al., Phys. Lett., 123B, (1983), 275.
(3) Bollini, D. et al., Nuovo Cimento, 63B, (1981), 441.
(4) Argento, A. et al., Phys. Lett., 120B, (1983), 245.
(5) Glashow, S.L., Salam, A. and Weinberg, S., Phys. Rev. Lett., 19, (1967), 1264.
(6) Bjorken, J.D., Phys. Rev., 148, (1966), 1467.
(7) Ellis, J. and Jaffe, R., Phys. Rev., D9, (1974), 1444.
(8) Darrigol, O. and Hayot, F., Nucl. Phys., B141, (1978), 391.
(9) Baum, G. et al., Phys. Rev. Lett., 51, (1983), 1135.

(10) Buras, A.J. and Gaemers, K.J.F., Nucl. Phys., B132, (1978), 249.
(11) Court, G.R., these proceedings.
(12) Close, F.E., Nucl. Phys., B80, (1974), 269.
(13) Look, G.W. and Fischbach, E., Phys. Rev., D16, (1977), 211.
(14) Karlitz, R. and Kaur, J., Phys. Rev. Lett., 38, (1977), 673.
(15) Jaffe, R.L., Phys. Rev., D11, (1975), 1953.
(16) Schwinger, J., Nucl. Phys., B123, (1977), 223.
(17) Preparata, G., High Energy Physics with Polarised Beams and Polarised Targets, edited by Joseph, C. and Soffer, J. (Birkhauser, Basel, 1981), 121.
(18) Kuti, J. and Weisskopf, V.F., Phys. Rev., D4, (1971), 3418.